

Evaluation of A PSI-Based Change Detection Regarding Simulation, Comparison, and Application

C. H. Yang *, U. Soergel

Institute for Photogrammetry, University of Stuttgart, Stuttgart, Germany - (yang, soergel@ifp.uni-stuttgart.de

KEY WORDS: Synthetic Aperture Radar (SAR), Persistent Scatterer Interferometry (PSI), Change Detection, Time Series Analysis, Urban Monitoring

ABSTRACT:

Persistent scatterer interferometry (PSI) detects and analyses strong, stable, and coherent radar signals throughout a time series of SAR images. Such coherent signals are reflected from corner-reflector-like substructures in built-up cities, which are regarded as so-called PS points. Certain PS properties such as deformation velocity and topography height can be derived for scene monitoring. Previously, we introduced a PSI-based change detection to detect disappearing and emerging PS points along with their occurrence times. Such temporary PS points existing only during a certain period correspond to change events, e.g., mostly constructions in cities. The tests using TerraSAR-X images successfully identified where and when the construction events in Berlin took place in 2013. The results were compared and all agreed with the ground truth. In this study, we evaluate our method more deeply. A simulation test is conducted to evaluate the theoretical accuracy in space and time. We also compare our method with two classical approaches: image rationing and amplitude-based semi-PS detection. The computational requirements are revealed afterwards. Finally, potential applications are proposed and discussed. All of these works help us to better characterize our technique and learn the pros and cons.

1. INTRODUCTION

Remote sensing techniques based on satellite images scan and map large areas in a cost-effective way compared with in situ surveys. Among them, spaceborne SAR sensors deliver radar images, which are acquired regularly over vast areas at fine spatiotemporal resolution. For example, TerraSAR-X operating in High-Resolution Spotlight Mode provides a new duplicate image every 11 days, which covers a specific area of 5 km × 5 km with around 1 m resolution. Such an image series are further used in interferometry techniques for scene monitoring. Moreover, active SAR sensors are weather independent and have a day-and-night vision ability. This advantage makes SAR images free of cloud occlusion and always available for use. These characteristics make SAR suitable for long-term monitoring tasks.

Among interferometry techniques, persistent scatterer interferometry (PSI) (Crosetto et al., 2016; Ferretti et al., 2000, 2001, 2011; Hooper et al., 2004; Kampes, 2006) detects strong, stable, and coherent radar signals from a SAR image stack. These signals are reflected from so-called persistent scatterer (PS) points on ground like building substructures. They are used to derive certain PS attributes such as temporal coherence, line-of-sight (LoS) velocity (mm/year level), topography height, geographic position, etc. for monitoring works. In practice, PSI works well in built-up cities because the preferred rectangular alignment of stationary structures ensures high PS density.

Nowadays, spaceborne SAR images have become easily accessible and more affordable for civil usage. Relevant applications are hence widened as well. One of them is oriented towards monitoring of man-made structures in detail with high-resolution SAR images, e.g., TerraSAR-X, COSMO-SkyMed, and PALSAR-2. Many fellows have improved and adapted PSI techniques to estimate structural deformation of buildings and infrastructures at small scale of millimeter or centimeter level

(Gernhardt and Bamler, 2012; Huang et al., 2017; Schunert and Soergel, 2016). In contrast, we are extending PSI to detect large-scale change events like building constructions.

Our previous work (Yang and Soergel, 2018) proposed a spatiotemporal change detection to recognize temporary PS points, which disappear or emerge at certain times. We distinguish and label these two point types as disappearing big change (DBC) and emerging big change (EBC) points. They are considered building changes in built-up areas. The core idea introduces a change index for each image pixel to qualify the probability of being a change point. We propose a statistics-based procedure to identify change points. The occurrence times are then located from the evolution of their change index sequences. Our test results successfully detected where and when the construction events in Berlin took place in 2013. They were all compared and agreed with the ground truth.

This study inspects our change detection method more deeply. We first conduct a simulation test to evaluate the theoretical accuracy in space and time. We learn where errors come from and how to avoid them. The real data test demonstrates a small test area in Berlin where many construction events occurred dynamically. This test site is also used in comparison with two classical approaches: image rationing and amplitude-based semi-PS detection (Ferretti et al., 2003). The comparison results highlight the advantages of our approach. We also address the computation requirements and the potential applications.

This paper is organized as follows. We first describe our change detection approach, image rationing, and amplitude-based semi-PS detection in Section 2. These three methods are later compared in Section 4, which follows the simulation test in Section 3. Section 5 talks about the applications that our method could be contributed to. The conclusions are finally summarized in Section 6.

* Corresponding author

2. METHODOLOGIES

2.1 Proposed Change Detection

We shortly review our PSI-based change detection (Yang and Soergel, 2018). To begin with, multi-temporal SAR images are divided into several subsets by a sequence of break dates (an interval between two successive image acquisitions). We want to detect the change events, which took place during these break dates. The temporal coherence of each pixel in each image set is estimated in a standard PSI processing. The change events must cause variation of temporal coherences over time. Simply speaking, when the time is passing forward, a disappearance or emergence event leads to decrease or increase of temporal coherences, respectively. The key idea is to derive a change index sequence for each pixel from the variation of its temporal coherence estimates across different periods. These change indices quantify probabilities of change events subject to a break date. The higher the change indices are, the more likely there are changes occurring. Change points are then extracted by statistical analysis on the change indices. We eliminate the blunders by spatial filters, which are designed based on spatial characteristics among change points. Finally, for each change point we check the evolution of its change index sequence to identify the occurrence date.

2.2 Image Rationing

The procedure used in this study refers to Rignot and van Zyl (1993). We first derived two intensity images (dB) from their original complex images. These two images were acquired at different times, in between the change events of interest occurred. Dividing the intensity images results in a ratio image. The ratio values of unchanged objects concentrate at 0 as a Gaussian distribution; in contrast, those of changed objects tend towards positives or negatives. Finally, we utilized Otsu thresholding (Otsu, 1979) to extract changes.

2.3 Amplitude-based Semi-PS Detection

The concept of semi-PS points was introduced by Ferretti et al. (2003). This method looks for abrupt amplitude changes of pixels in a SAR image stack to recognize semi-PS points. A step detector can be utilized for this purpose. These semi-PS points are then referred to changes such as construction events in urban areas. For instance, a group of pixels is considered a new building if they manifest brighter in an image sequence after a specific date. In contrast, pixels, which become darker, are regarded as torn-down buildings. In this study, we adapt the procedure of semi-PS detection to be comparable to our approach. Both methods have the similar concept. The main difference is that ours uses phase signals of SAR images but another used amplitude signals of them.

3. SIMULATION TEST

3.1 Simulation Procedure

A time series of M interferograms is simulated, where PS, DBC, EBC, and Void points are randomly distributed. This simulation assumes perfect PSI processing and considers only random noise. A stochastic constant phase φ_{cons} is assigned to the simulated phases $\varphi_{\text{sim}}^{\text{int}} [-\pi, \pi) \in \mathbb{R}$ of each pixel x :

$$\varphi_{\text{sim}}^{\text{int}}(x) = \varphi_{\text{cons}}(x), \text{int} = [1, M]. \quad (1)$$

Gaussian phase noise $\varphi_n^{\text{int}} (\mu = 0, \sigma = [-\pi, \pi) \in \mathbb{R})$ is then added to the simulated phases:

$$\varphi_{\text{sim}}^{\text{int}}(x) = \varphi_{\text{cons}}(x) + \varphi_n^{\text{int}}(x). \quad (2)$$

The temporal coherences of $\varphi_{\text{sim}}^{\text{int}}(x)$ are calculated by

$$\gamma_T(x) = \left| \frac{1}{M} \cdot \sum_{j \in [0, 1] \in \mathbb{R}} \exp(j \cdot \varphi_{\text{sim}}^{\text{int}}(x)) \right|. \quad (3)$$

Pixels are selected as PS points if their temporal coherences fulfil a specified threshold. Among them, in case a DBC or EBC point disappears or emerges right after a break date (bd), a series of irregular phases $\varphi_{\text{irr}}^{\text{int}^D}$ or $\varphi_{\text{irr}}^{\text{int}^E}$ is added to its simulated phases as

$$\varphi_{\text{sim}}^{\text{int}}(x) = \varphi_{\text{cons}}(x) + \varphi_n^{\text{int}}(x) + \varphi_{\text{irr}}^{\text{int}^D}(x), \text{int}^D = [bd + 1, M] \quad (4)$$

$$\varphi_{\text{sim}}^{\text{int}}(x) = \varphi_{\text{cons}}(x) + \varphi_n^{\text{int}}(x) + \varphi_{\text{irr}}^{\text{int}^E}(x), \text{int}^E = [1, bd] \quad (5)$$

respectively. Finally, those pixels without any label are regarded as void points.

3.2 Simulated Data

We simulated a scene like a developing city with numerous big changes (more than 30% coverage) to analyse the performance of our approach. For this purpose, we generated 81 SAR images containing 58% PS, 17% DBC, 17% EBC, and 8% void points (Figure 1). A temporal coherence threshold of 0.8 (Yang and Soergel, 2018) is used for PS selection. The disappearance and emergence dates of the change points are evenly distributed to the middle period from break dates 31 to 51.

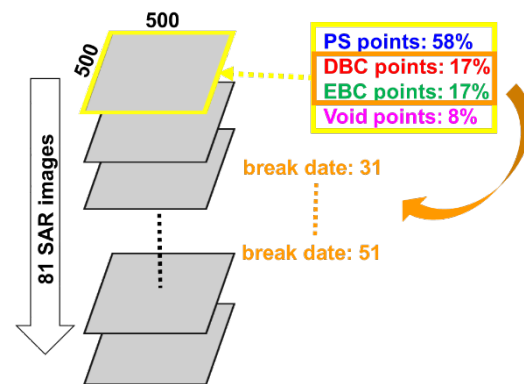


Figure 1. Simulated data

3.3 Accuracy Assessment

Our approach is used to detect the positions of different point labels and to estimate the occurrence break dates of change points. We assess the detection accuracy by using confusion matrix (Table 1). The overall accuracy is 99% and all of the producer's and user's accuracies are better than 99%. Such high accuracy tells that our approach works well given perfect PSI computations. In this test, we assume that those PSI-related phase noises caused by residual topographic errors, atmospheric effect, orbital inaccuracy, flat Earth, temporal and geometric decorrelations, and image processing, are perfectly calibrated or removed. In practice, they must be delicately handled in a PSI processing for an accurate result. This is not an easy task and requires deep expertise and experience. We do not dig into the details in this study.

		Reference				
		PS	DBC	EBC	Void	Sum
Result	PS	145544	110	93	0	145747
	DBC	0	41647	0	0	41647
	EBC	0	0	41713	0	41713
	Void	0	0	0	20893	20893
	Sum	145544	41757	41806	20899	250000
		PS	DBC	EBC	Void	
Producer's Accuracy		100%	99%	99%	100%	
User's Accuracy		99%	100%	100%	100%	
Overall Accuracy		99%				

Table 1. Confusion matrix

The only errors are the change points that are falsely labelled as PS. This results in producer's accuracy of 99% for both change labels and user's accuracy of 99% for PS. Such an error often happens if a change point emerged very early or disappeared very late. In this case, its temporal coherence, which is evaluated from the whole images, is still above the threshold to be wrongly selected as a PS point. The reason is that those images, in which the change points act as PS points after emergence or before disappearance, account for a large proportion of the whole images. Consequently, they turn out to be false PS points, which are missed detections of change points. This problem can be solved by using sufficient images.

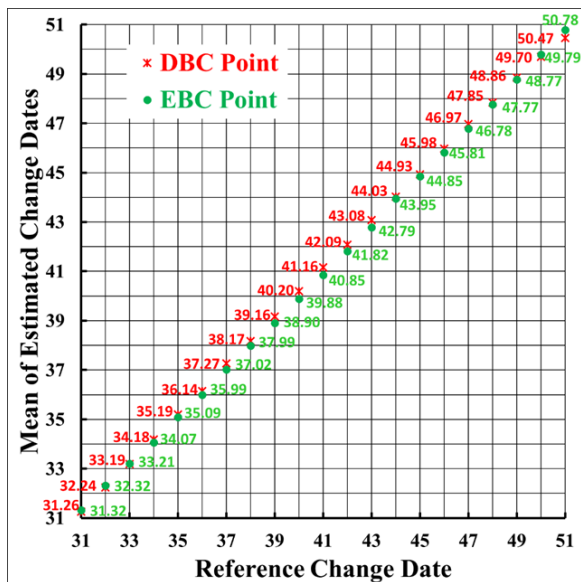


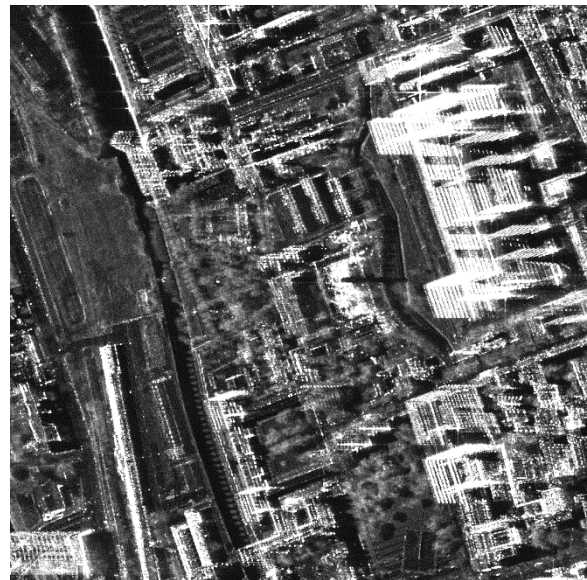
Figure 2. Mean of estimated change dates versus each reference change date.

To access the temporal accuracy, the estimated change dates are compared with the reference (Figure 2). For each reference change date, we calculate the mean of the estimated disappearance dates (red) and plot it in the vertical axis. The correlation coefficient is 0.999, indicating a high agreement between the estimated and reference disappearance dates. The mean absolute difference is 0.17 and the maximum absolute difference is 0.53. The accuracy of estimated disappearance date thus achieves sublevel of break date. That is to say, given Sentinel-1 images, the accuracy could be shorter than 6 days

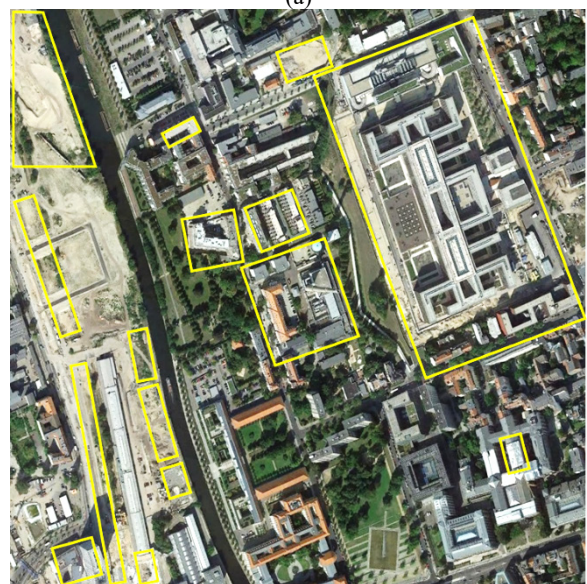
(shortest temporal baseline) under optimal conditions, i.e., sufficient images and high-quality PSI processing. The estimated emergence dates (green) show the same characteristics as the disappearance case. The correlation coefficient is also 0.999. The mean absolute difference is 0.16 and the maximum absolute difference is 0.32. In summary, we prove that given optimal conditions our method is able to detect events' occurrence times with a considerably high accuracy.

4. REAL DATA TEST

4.1 Test results



(a)



(b)

Figure 3. Study area at the north of Berlin Central Station. (a) Mean TerraSAR-X image. (b) Aerial image (Google Earth) acquired on September 5, 2014. Yellow square, building construction.

Our test area is located at the north of Berlin Central Station (Figure 3). The mean TerraSAR-X image (Figure 3(a)) shows many bright clusters of strong signals, which appear to be potential PS and change points. The yellow squares in the aerial image (Figure 3(b)) indicates the construction events taking place

in 2013. We adopted forty TerraSAR-X images for our test, which were acquired in High-Resolution Spotlight Mode from October 27, 2010 to September 4, 2014. All of the images were precisely co-registered and resampled into 5000×5000 grid (ground resolution: 1m). The test result (Figure 4) successfully identifies where and when the change events occurred. All of the events were compared and all agree with the ground truth (Yang and Soergel, 2018).

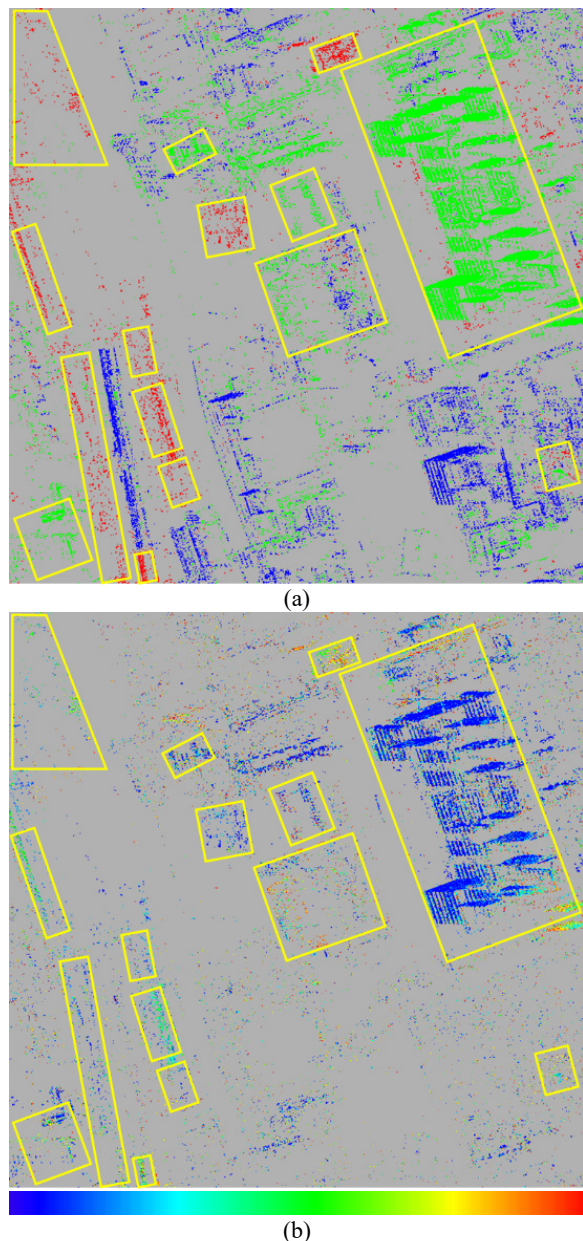


Figure 4. Spatiotemporal change detection result. (a) Steady, disappearing, and emerging structures represented by PS (blue), DBC (red), and EBC (green) points. (b) Occurrence dates: blue to red, earliest to latest in 2013. Yellow square, building construction.

4.2 Comparison with ratio change detection

The ratio image (Figure 5(a)) manifests the potential changes highlighted by extreme values towards black and red. Among the detected changes (Figure 5(b)) we can identify those clusters subject to building constructions. However, we also observe salt-and-pepper noise over the scene, which stem from speckle and

image noise. Both correct and false results are mixed, which leads to difficulty in interpretation. To diminish the impact of speckle, we applied Lee speckle filtering (Lee, 1981) of size 5×5 to the intensity images before ratioing in the second experiment. The changes due to construction (Figure 6) can be more clearly identified; however, the false alarms, in particular noise, still dominate the result. Finally, we turned to multi-looking by a factor of 100 before ratioing to reduce both speckle and image noise in the intensity images. As a result, most false alarms have been eliminated (Figure 7). Nevertheless, we lose rather spatial details.

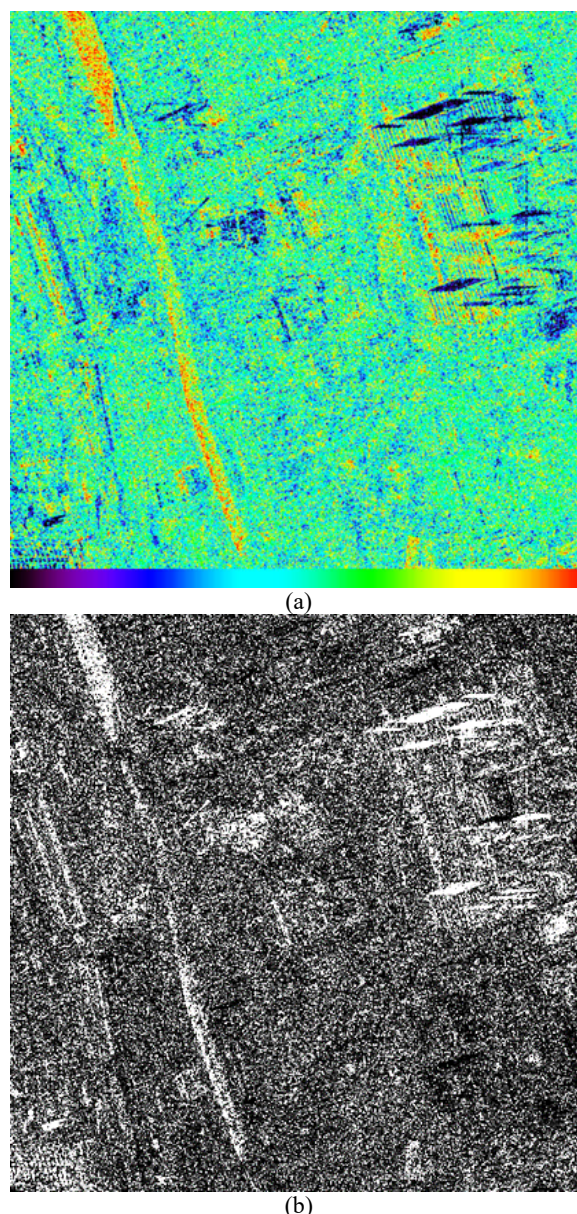
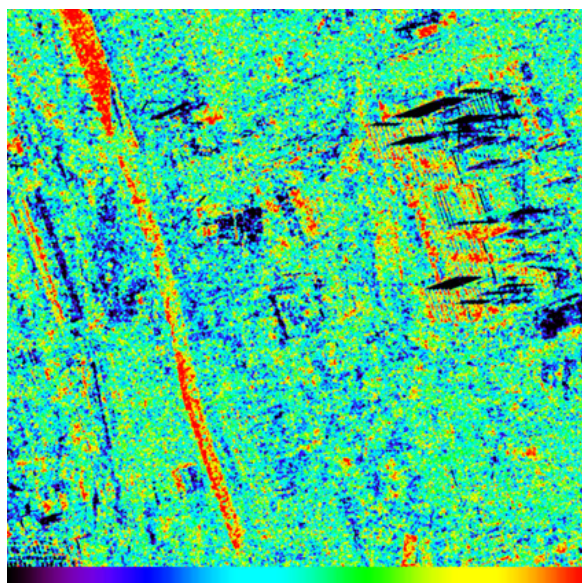
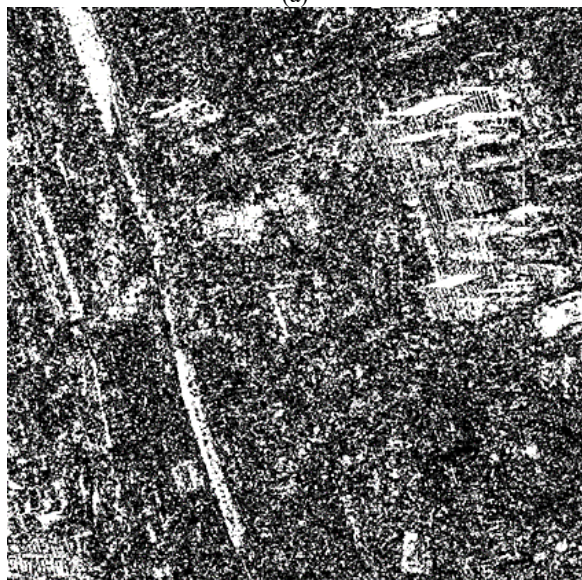


Figure 5. Original example. (a) Ratio image (potential changes towards black and red). (b) Detected changes (white).



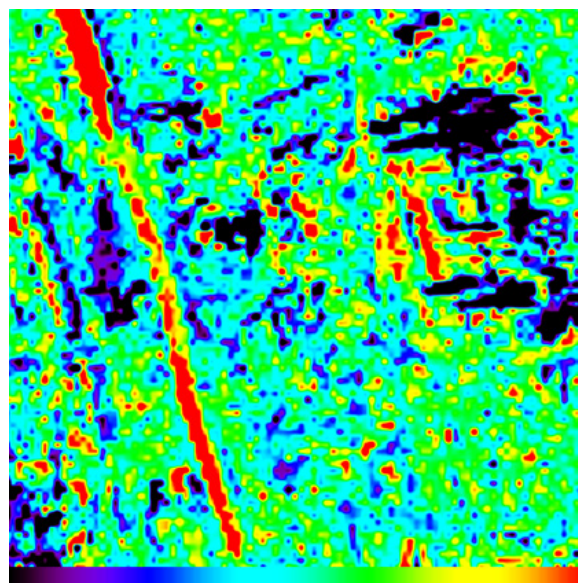
(a)



(b)

Figure 6. Despeckle example. (a) Ratio image (potential changes towards black and red). (b) Detected changes (white).

The problems mentioned above exist not only for ratio change detection but also for other incoherent approaches (Preiss and Stacy, 2006). Another common problem is that different change types are not easily discriminated. The strategy of our method looks for disappearance and emergence of PS points. Five advantages are listed in the following. First, the delivered change information regards space, where, and time, when. Second, steady structures and change events are clearly identified and distinguished. Third, irrelevant changes like vegetation growth are automatically excluded. Fourth, full-resolution details are preserved. Last but not least, speckle and noise are ignored.



(a)



(b)

Figure 7. Multi-looking example. (a) Ratio image (potential changes towards black and red). (b) Detected changes (white).

4.3 Comparison with amplitude-based semi-PS detection

We tailor the method proposed in Ferretti et al. (2003) to detect the construction events (semi-PS points) that occurred in our study area in 2013 (Figure 8). Our comparison (Figures 4(a) vs 8) reveals that the DBC and EBC points are increased by 223% and 498% in our approach. The amplitude-based result loses partial details or even entire change events. The change points are too few to provide complete information of changes. For example, most of the EBC points are missing in the centre yellow square, which fails to convey the renovation activity. In addition, the clustered EBC points (a new government office) in the top-right square becomes very sparse. We also see many of the DBC points on the left side are missing. In summary, our approach working on phase information has proven capable of detecting more change points, i.e., more complete change information.

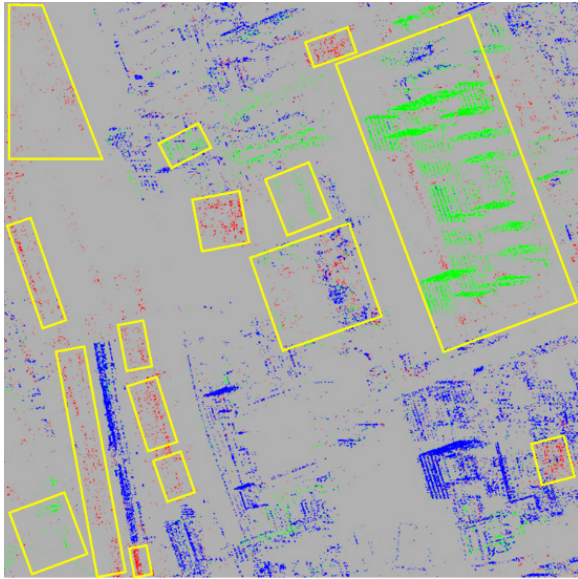


Figure 8. Amplitude-based semi-PS result. Steady, disappearing, and emerging structures represented by PS (blue), DBC (red), and EBC (green) points. Yellow square, building construction.

4.4 Computational requirements

The proposed approach was running on a computer with Intel Core(TM) i7-5820K, CPU running at 3.30 GHz, and 64GB RAM. The computational demand is divided into two parts. The heavier part is attributed to PSI processes, each of which takes hours to days or even longer depending on the size of data and PSI-related parameters. The second part belongs to change detection step (our main contribution) and only takes minutes after inputs generated by PSI are read. We have seen two prospects to speed up time-consuming PSI processing. First, the computing power of CPU always keeps increasing. With advanced techniques, e.g., parallel computing, we believe that the time required for PSI computations will be significantly shortened. This enables our approach to be near real-time or even real-time monitoring. Second, the PSI procedure can be simplified if accurate complementary data and a priori knowledge are available. For example, deformation velocities and residual heights, which are usually estimated in PSI, can be preset to null under two conditions. First, the areas of interest area are steady without noticeable movement. Second, accurate DEM data are used to compensate for topography. This preset dramatically reduces computing times.

5. APPLICABILITY

Our method is particularly suitable to monitor built-up areas, where many PS and change points, if any, can be found. For instance, we can distinguish destroyed and damaged buildings due to natural disasters (e.g., earthquake) from the construction events happening before. The subsequent reconstruction can then be monitored as well.

As mentioned before, in urban areas only structural changes can be detected but what kinds of them, e.g., facades, roofs, houses, offices, factories, or infrastructures. We can utilize GIS-based information, like 3D city models or topic maps, to label change points and bring semantic products. For this purpose, points should be first clustered and segmented depending on their properties such as labels, spatial proximity, occurrence times,

geometry, homogeneity, temporal coherences, and so on. An ideal service would be an interactive platform to convey spatiotemporal change information.

Our technique can be upgraded to detect a new change point label, which undergoes double big changes during a certain period. For instance, a new building was erected soon, following a demolition event at the same venue. To this end, change index sequences must be processed more deeply. A pixel will be marked and further analysed if its change indices indicate a pattern subject to double changes.

We can adapt the current method for distributed scatterers (DS) points. This adapted version enables changes on natural objects, such as rocky terrain overwhelmed by magma, to be identified. Another idea is to monitor underground activities like tunneling. Normally such events speed up sinking velocities of PS points upon the surface. We could create another kind of change indices from such velocity variation. Afterwards the concept of the current approach can be realized to detect underground constructions.

6. CONCLUSIONS

Previously, we proposed a PSI-based method to detect where and when change events like constructions occurred. In this study, we evaluate our method more deeply by concerning the detection accuracy in space and time. The simulation test proves that our approach is very accurate given optimal conditions and perfect PSI processing. The detection accuracy of change points is accessed by confusion matrix. The overall accuracy is 99% and all of the producer's and user's accuracies are higher than 99%. The temporal accuracy achieves sublevel between two consecutive images. For example, the temporal accuracy given use of Sentinel-1 images could be shorter than 6 days.

Compared with incoherent change detection, our technique has five advantages because only PS-like signals are involved in processing. First, the delivered change information regards space, where, and time, when. Second, steady structures and change events are clearly identified and distinguished. Third, irrelevant changes like vegetation growth are intrinsically excluded. Fourth, full-resolution details are preserved. Finally yet importantly, speckle and noise are ignored. We also made comparison with a similar amplitude-based method. Our phase-based approach proves able to detect more change points, which convey complete change information.

We share some ideas about applications, regarding disaster monitoring, GIS-based interactive platform, multiple changes at the same site, natural scene change, and detection of underground activities. There are many potential applications promising in the future with two perspectives. First, the computing power of CPU is increasing. Second, more and more advanced SAR sensors will be launched and in operation for civil usage with affordable or free charge.

REFERENCES

- Crosetto, M., Monserrat, O., Cuevas-González, M., Devanthery, N. and Crippa, B., 2016. Persistent scatterer interferometry: a review. *ISPRS Journal of Photogrammetry and Remote Sensing*, 115, 78-89.
- Ferretti, A., Prati, C. and Rocca, F., 2000. Nonlinear subsidence rate estimation using permanent scatterers in differential SAR

interferometry. *IEEE Transactions on Geoscience and Remote Sensing*, 38(5), 2202-2212.

Ferretti, A., Prati, C. and Rocca, F., 2001. Permanent scatterers in SAR interferometry. *IEEE Transactions on Geoscience and Remote Sensing*, 39(1), 8-20.

Ferretti, A., Colesanti, C., Perissin, D., Prati, C. and Rocca, F., 2003. Evaluating the effect of the observation time on the distribution of SAR permanent scatterers, *FRINGE 2003*.

Ferretti, A., Fumagalli, A., Novali, A., Prati, C., Rocca, F. and Rucci, A., 2011. A new algorithm for processing interferometric data-stacks: SqueeSAR. *IEEE Transactions on Geoscience and Remote Sensing*, 49(9), 3460-3470.

Gernhardt, S. and Bamler, R., 2012. Deformation monitoring of single buildings using meter-resolution SAR data in PSI. *ISPRS Journal of Photogrammetry and Remote Sensing*, 115, 68-79.

Hooper, A., Zebker, H., Segall, P. and Kampes, B., 2004. A new method for measuring deformation on volcanoes and other natural terrains using InSAR persistent scatterers. *Geophysical Research Letters*, 31(23), 1-5.

Huang, Q., Crosetto, M., Monserrat, O. and Crippa, B., 2017. Displacement monitoring and modelling of a high-speed railway bridge using C-band Sentinel-1 data. *ISPRS Journal of Photogrammetry and Remote Sensing*, 128, 204-211.

Kampes, M., 2006. *Radar Interferometry: Persistent Scatterer Technique*. Springer.

Lee, J.S., 1981. Refined filtering of image noise using local statistics. *Computer Graphics and Image Processing*, 15(4), 380-389.

Otsu, N., 1979. A threshold selection method from gray-level histograms. *IEEE Transactions on Systems, Man, and Cybernetics: Systems*, 9, 62-66.

Preiss, M. and Stacy, N.J.S., 2006. *Coherent Change Detection: Theoretical Description and Experimental Results*. Defence Science and Technology Organisation.

Rignot, E.J.M. and van Zyl, J.J., 1993. Change detection techniques for ERS-1 SAR Data. *IEEE Trans. IEEE Transactions on Geoscience and Remote Sensing*, 31, 896-906.

Schunert, A. and Soergel, U., 2016. Assignment of persistent scatterers to buildings. *IEEE Transactions on Geoscience and Remote Sensing*, 54(6), 3116-3127.

Yang, C.-H. and Soergel, U., 2018. Adaptive 4D PSI-based change detection. *ISPRS Ann. Photogramm. Remote Sens. Spatial Inf. Sci.*, IV-3, 245-250, <https://doi.org/10.5194/isprs-annals-IV-3-245-2018>.